

1 Article

2 Removal of Various Pollutants from Wastewaters Using an 3 Efficient and Degradable Hypercrosslinked Polymer

4 Zujin Yang^{1,3}, Yuxin Chai¹, Qiuru Li², Hongbing Ji^{2,3,4*}5 ¹ School of Chemical Engineering and Technology, Sun Yat-sen University, Zhuhai 519082, China;
6 yangzj3@mail.sysu.edu.cn; yuxin_1230@qq.com7 ² Fine Chemical Industry Research Institute, The Key Laboratory of Low-carbon Chemistry & Energy
8 Conservation of Guangdong Province, School of Chemistry, Sun Yat-sen University, Guangzhou 510275, China;
9 jihb@mail.sysu.edu.cn; 1045757624@qq.com10 ³ Huizhou Research Institute of Sun Yat-sen University, Huizhou 516216, China; yangzj3@mail.sysu.edu.cn;
11 jihb@mail.sysu.edu.cn12 ⁴ School of Chemical Engineering, Guangdong University of Petrochemical Technology, Maomen 525000,
13 China; jihb@mail.sysu.edu.cn

14 * Correspondence: jihb@mail.sysu.edu.cn; Tel.: +86 20 84113658

15
16 **Abstract:** Adsorption is an effective strategy for the removal of pollutants from the wastewater. Herein,
17 a 2-hydroxyterephthalic acid (HTC) modified hypercrosslinked polymer (HTC-HCP) is successfully
18 synthesized via Friedel-Crafts reactions, and used as an adsorbent for the different types of pollutants
19 including organic contaminants and heavy metal ions from wastewater. Excellent adsorption capacities are
20 observed for amines (aniline, *p*-methylaniline (*p*-MA), *p*-chloroaniline (*p*-CA), and *p*-aminobenzoic acid
21 (*p*-ABA)), phenols (phenol, *p*-chlorophenol (4-CP) Bisphenol A (BPA), 1-Naphthol (1-NP)), dyes (rhodamine
22 B (RhB) and methyl orange (MO)), and metal ions (Pb²⁺, Hg²⁺, and Cd²⁺). The resulting polymers exhibited
23 excellent adsorption performance towards these pollutants. Especially, the removal rate of aniline is above 95%
24 in the concentration of 2.5 mg/L in 40 min at 25 °C. The interaction mechanism has been investigated, and
25 confirmed by FTIR and the theoretical calculation results. It is due to surface complexation and chemisorption
26 between adsorbent and adsorbate. The polymer exhibits good performance such as high adsorption capacity,
27 high separation efficiency, biodegradable properties, and easy regeneration, suggesting that its potential
28 technological applications for the removal of organic compounds and heavy metal ions from actual industrial
29 effluent.

30 **Keywords:** Hypercrosslinked polymer; *p*-hydroxy-phthalic acid; pollutants; adsorption; biodegradation31
32

1. Introduction

33 Water pollution caused by toxic organic chemicals and heavy metal ions has aroused global attention
34 because of their adverse influence to human health and the environment [1, 2]. For the sustainable development
35 of water environment, it has become a very urgent concern to develop new efficient methods to remove the
36 compounds from wastewater [3, 4]. Many methods have been developed for the removal of organic pollutants
37 and heavy metal ions including chemical precipitation, photocatalytic degradation, biodegradation, membrane
38 filtration, and adsorption [5-10]. Among these methods, adsorption is an effective, efficient, and economic
39 method for the removal of pollutants from wastewaters due to its low cost, easy operation, and practical
40 application in large scale [11]. In recent years, polymeric sorbents have been widely studied as adsorbents
41 because of their obvious advantages including good mechanical strength, easy modified properties, and
42 feasible regeneration [12, 13]. In comparison, hypercrosslinked polymers (HCPs) are more efficient for
43 adsorption of pollutants due to their high specific surface areas, favorable pore structures, and excellent
44 adsorption performance [14-17]. Generally, HCPs can be prepared from linear polystyrene or low cross-linked
45 polystyrene by Friedel-Crafts reaction under the help of catalyst [18]. However, in review of the previous refs,
46 the as-synthesized HCPs show relatively low performance toward the pollutants [14-16]. Therefore, it is
47 necessary to introduce some special groups on the polymers by chemical modification to improve their

48 adsorption selectivity towards these pollutants from wastewater. Adsorbents containing amino, amide,
49 hydroxyl, and carbonyl groups have been applied for the removal of organic pollutants and heavy metal ions
50 from wastewater [16, 19-21].

51 2-hydroxyterephthalic acid (HTC), has been used extensively in medicine and functional materials [22].
52 HTC contains the -OH and -COOH groups, which are used to improve adsorption selectivity of the polymers. It
53 is grafted onto the surface of HCPs to form surface complexation, acid-base complex, and hydrogen bonding in
54 the limited micro domains, which greatly enhance the adsorption performance towards pollutants. However,
55 for the waste synthetic polymers such as polyethylene, polystyrene, and polypropylene, environmental
56 pollution has been a serious problem due to their nonbiodegradability. Therefore, studying biodegradable
57 materials including a fully or partially biodegradable film or resin has been the focus of much research over
58 the past two decades. However, little literature was published in the previously reported refs about HTC-HCP
59 on how to enhance sorption of different types of pollutants including toxic organic chemicals and heavy metal
60 ions from aqueous solution and their biodegradability so far.

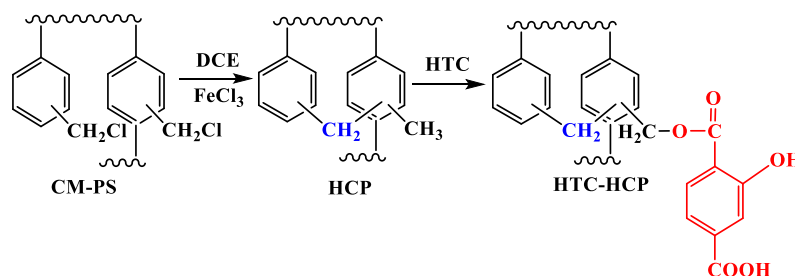
61 The objective of this work is to synthesize a polar monomer HTC modified HCP (HTC-HCP) for the
62 removal of organic pollutants and heavy metal ions from wastewater. Its surface chemistry and structure are
63 characterized by using Scanning electron microscopy (SEM), Fourier transform infrared spectroscopy (FTIR),
64 Thermogravimetric analysis (TGA), X-ray photoelectron spectroscopy (XPS), and N₂ adsorption-desorption
65 measurements. The resulting HTC-HCP can remove various organic pollutants, such as dyes, amines and
66 phenols, and metal ions like Pb²⁺, Hg²⁺, and Cd²⁺ from aqueous solutions. Biodegradation experiment is also
67 tested. Finally, a possible adsorption mechanism is proposed based on the experimental and computational
68 results. It provides an industrialized application as a reference for the removal of aniline components and heavy
69 metal ions from industrial wastewater.

70 2. Materials and Methods

71 2.1. Synthesis of HTC-HCP

72 As described in Scheme 1, HTC-HCP was synthesized according to previous works with minor
73 modification [23, 24]. 10 g of chloromethylated poly(styrene-co-divinylbenzene) (CM-PS) beads was
74 first dispersed in 50 mL of 1,2-dichloroethane (DCE) to swell overnight. About 2 g of anhydrous
75 FeCl₃ as catalyst was added to the system and stirred until the catalyst was completely dissolved.
76 Then, the reaction mixture was heated to 115 °C within 1.5 h and kept the same temperature for 12 h.
77 After the reaction was finished, the product was filtered and washed alternately with 1% aqueous
78 hydrochloric acid and 95% (v/v) ethanol until pH of the washings was neutral, and finally dried
79 under vacuum at 80 °C for 12 h to acquire HCP. After that, 2.5 g of the above as-prepared HCP was
80 mixed with 60 mL of N,N-dimethylformamide (DMF) containing 1.0 g of HTC, and the reaction
81 mixture was maintained at 115 °C for 12 h with N₂ protection. The reaction mixture was separated
82 by filtration, washed with deionized water until neutral pH, and the corresponding HTC-HCP was
83 further purified by Soxhlet extraction with ethanol for 24 h and dried in vacuum to obtain the final
84 product.

85



86

87

Scheme 1. The synthesis procedure of HTC-HCP

88

88 2.2. characterization

89

90

91

92

The chlorine content in the polymers was calculated according to the Volhard method^[25]. FTIR spectra of the polymers were recorded on a Fourier transform infrared spectrometer (Perkin-Elmer 2000, USA) using KBr as background over the range of 4000–400 cm⁻¹ under ambient conditions. TGA of HTC-HCP was performed on a Netzsch STA-449C thermal analysis system (Netzsch,

93 Germany). For TG measurements, the weight loss of dried samples was monitored under N₂
 94 atmosphere from room temperature to 850 °C at a rate of 10 °C/min.. The BET surface area and pore
 95 distribution of the polymers were analyzed by nitrogen adsorption-desorption isotherm at 77 K in a
 96 Micromeritics ASAP 2020 accelerated surface area and porosimetry analyzer (Micromeritics,
 97 Norcross, GA, USA). XPS (Thermo, ESCALAB 250XI, USA) was used to determine the electron
 98 binding energy of the surface to achieve the qualitative analysis of the elements. To detect surface
 99 properties of the hydrophobic polymers in aqueous phase, their contact angles were recorded with a
 100 contact angle measuring system (OCA20, Dataphysics, Germany).

101 2.3. Adsorption experiments

102 Adsorption was carried out with dyes (RB and MO), amines (aniline, *p*-MA, *p*-CA, and *p*-ABA),
 103 or phenols (phenol, 4-CP, BPA, 1-NP) at a desired temperature and an agitation speed of 200 r/min
 104 until the equilibrium. 0.1 g of HTC-HCP was mixed 100 mL of solution containing initial
 105 concentration 100 mg/L of organic compounds in a 250 mL a conical flask. The reaction mixture was
 106 shaken at 25 °C. During the adsorption, 0.5 mL of the solution was sampled at regular intervals, and
 107 transferred to a 10 mL volumetric flask and diluted with water to the volume. After that, the
 108 samples were determined by UV-Vis spectroscopy until adsorption equilibrium was reached.

109 Adsorption of metal ions was performed in a 100 mL Pb²⁺, Hg²⁺, and Cd²⁺ aqueous solution
 110 (concentration 100 mg/L) at 25 °C with 0.1 g HTC-HCP. 0.5 mL of supernatant was taken at intervals.
 111 The supernatant samples of Pb²⁺ and Cd²⁺ was diluted to 5 mL and analyzed by atomic absorption
 112 spectrometry (AAS), and the supernatant samples of Hg²⁺ were diluted for 50 times, and analyzed
 113 by ICP-AES.

114 The adsorption amount of the organic pollutants and heavy metal ions at a contact time *t* was
 115 expressed as:

$$q_t = (C_o - C_t)V_0 / W \quad (1)$$

116

117 where q_t is the adsorption amount at contact time *t* (mg/g resin); C_t is the concentration of each
 118 compound in solution at *t* (mg/L). All the experiments were performed in triplicate. The average
 119 values were reported and all standard errors were smaller than 5%.

120 For equilibrium adsorption, 0.1 g of HTC-HCP was mixed 100 mL of solution containing initial
 121 concentration 2-1000 mg/L of aniline in a 250 mL a conical flask. The reaction mixture was shaken at
 122 a desired temperature (25, 30, and 35 °C) and an agitation speed of 200 r/min until the equilibrium
 123 in 24 h. The original solution pH of aniline used in the equilibrium adsorption was adjusted with 0.1
 124 mol/L hydrochloric acid or 0.1 mol/L sodium hydroxide. The concentration of the aniline was
 125 measured by UV-Visible spectrometer. Based on the working curve, the adsorbed amount of aniline
 126 at the equilibrium was calculated as Eq (1).

127 2.4. Biodegradation experiments

128

129 A certain amount of CM-PS and HTC-HCP are dried to constant weight in a vacuum oven at
 130 70 °C for 24 h. A certain amount of dried CM-PS (w_1) and HTC-HCP (w_2) was mixed with some soil
 131 containing a stain, which was identified as *Stenotrophomonas sp.*, respectively. The degradation of
 132 adsorbents were studied by shaking flask culture at 30 °C. After shaking culture with the initial
 133 concentration of HTC in the solution being about 15 mg/L, the samples were withdrawn at 2 d
 134 intervals until the weight was constant . Therefore, CM-PS (w_1') and HTC-HCP (w_2') were obtained,
 135 and the degraded ratio (%) could be calculated as follows:

$$CM-PS(\%) = ((w_1 - w_1') / w_1) \times 100\% \quad (2)$$

$$HTC-HCP(\%) = ((w_2 - w_2') / w_2) \times 100\% \quad (3)$$

136 2.5. Computational chemistry calculations

137 Quantum calculations are usually used to examine the formation of chemical bonds between
 138 the adsorbate and adsorbent at the molecular level, which can yield some information on the
 139 structure and energy. The intermolecular interaction was modeled by calculating the hydrogen
 140 bond distances and complexation energies between aniline and HTC-HCP. In the present work, a

141 basic assumption was proposed that the binding sites in the polymer are HTC of HTC-HCP
 142 connected with aniline. The feasibility of the simulation with the similar structures has been
 143 reported in the literature [26]. In addition, the high convergence option was considered as the
 144 energy minimization of each model in aqueous media.

145 Binding energy (BE) could be expressed as

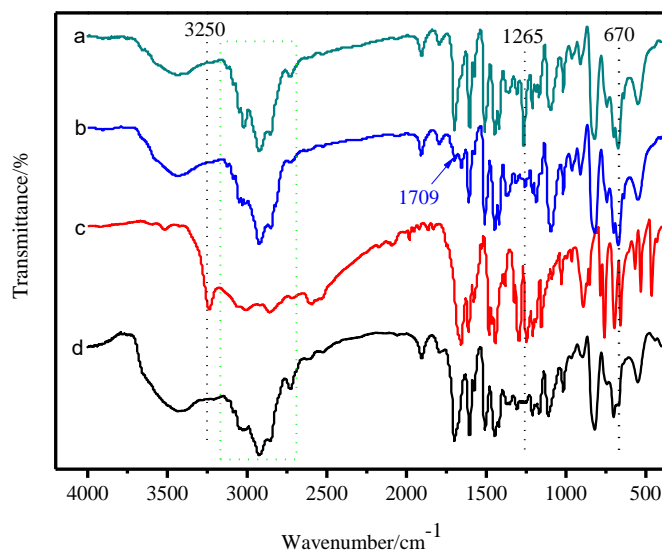
$$BE = E_{\text{complex}} - E_{\text{guest}} - E_{\text{host}} \quad (4)$$

146 E_{complex} is the total energies of the inclusion complex of aniline with HTC. E_{guest} is the sum of total
 147 energy of aniline. E_{host} is the total energy of HTC. The more negative the binding energy is, the more
 148 thermodynamically favorable the inclusion complex is.

149 3. Results and Discussion

150 3.1. Characterization of HTC-HCP

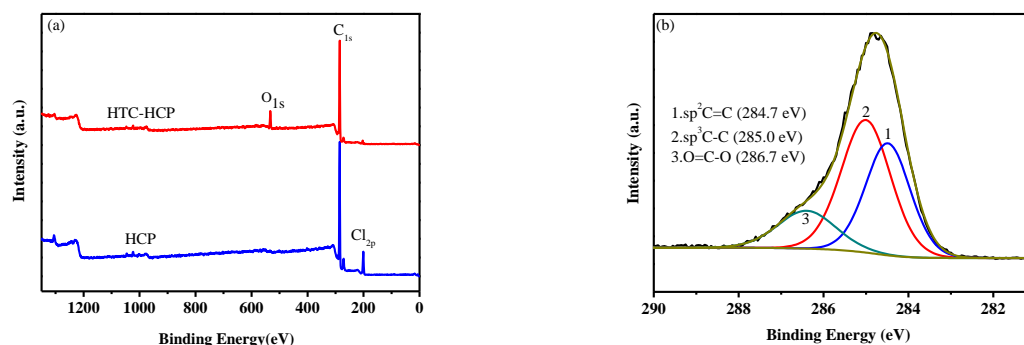
151 Fig.1 shows the FTIR spectra of the CM-PS, HCP, HTC, and HTC-HCP in the wavenumber
 152 range of 4000-400 cm^{-1} . For CM-PS, the bands due to the C-Cl stretching vibration of the $-\text{CH}_2\text{Cl}$
 153 groups are observed at 1265 cm^{-1} and 670 cm^{-1} [27] (Fig.1a). After the Friedel-Craft reaction, the peak
 154 at 1265 cm^{-1} is significantly weakened in HCP (Fig.1b). As seen in Fig.1c, the characteristic band at
 155 3250 cm^{-1} is due to $-\text{OH}$ stretching vibration, and the strong adsorption peak at 1706 cm^{-1} is ascribed
 156 to the carbonyl groups of HTC [22]. After the reaction of HTC with HCP, the peaks at 1265 and 670
 157 cm^{-1} almost disappear and the peak at 1706 cm^{-1} is also present for HTC-HCP (Fig.1d). In addition,
 158 a strong peak due to the $-\text{OH}$ stretching of HTC also appears at 3400 cm^{-1} . Table 1 shows that chlorine
 159 content for HCP (7.61%) is lower than that of CM-PS (18.32%). The residual chlorine content for
 160 HTC-HCP decreases from 12.61% to 0.21% after the reaction, revealing the reduction of $-\text{CH}_2\text{Cl}$
 161 groups as it reacts with the neighboring aromatic rings of HTC and transformed to the rigid
 162 methylene cross-linking bridges [28]. These results indicate that HTC was successfully introduced
 163 into HCP.
 164



165

166 **Fig. 1.** FTIR spectra of CM-PS (a), HCP (b), HTC (c), and HTC-HCP(d).

167 The surface chemical compositions and their changes of HCP and HTC-HCP are analyzed by
 168 XPS [29]. As shown in Fig.2a, the respective XPS wide scan of HCP and HTC-HCP shows that the O_{1s}
 169 peak of HTC-HCP is at 532.7 eV, while the Cl_{2p} peak almost disappears completely for HTC-HCP,
 170 suggesting $-\text{CH}_2\text{Cl}$ groups are involved in the reaction with HTC. As shown in Fig.2b, HTC-HCP
 171 has three different chemically shifted components [30, 31]: sp^2 C=C (284.7 eV), sp^3 C-C (285.0 eV), and
 172 O=C-O (286.7 eV). This phenomenon could be attributed to the fact that HTC possesses high ratio of
 173 C=C, C-C, and O=C-O in their structure, implying the presence of HTC on the surface of HCP.
 174



175 **Fig. 2.** XPS wide scan of (a) HCP and HTC-HCP; (b) C1s XPS spectra of HTC-HCP.

176 TGA shows that the thermal decomposition temperature of HTC-HCP is up to 180 °C under
 177 nitrogen atmosphere, the 13% mass loss in the range 180-450 °C is due to heat decomposition of HTC,
 178 and HTC-HCP retains about 28% mass at the temperature above 800 °C (**Figure S1**), implying the
 179 high thermal stability because of the highly crosslinked network of the polymer [32, 33]. Such a high
 180 thermal stability could be beneficial for the regeneration of adsorbent in practical applications. To
 181 analyze the polarity, the elemental analysis and the contact angle were carried out to analyze the
 182 polymers. As shown in **Table 1**, the O content of HTC-HCP is 4.98%, but its contact angle is 124°,
 183 which is lower than that observed for HCP (142°). This difference may be caused by the addition of
 184 HTC onto the surface of HCP, which improve hydrophilicity. These results indicate that the
 185 uploaded -COOH and -OH groups of HTC onto HCP is beneficial for the adsorption of organic
 186 contaminants.

187

Table1. Characterization of HTC-HCP

Materials	Surface		Pore volume (cm ³ /g)	Average pore size (nm)	Chlorine content (%)	O content (%)	Contact angle (deg)
	area(m ² /g)						
	S _{BET}	S _{micro}					
CM-PS	40.25	3.53	0.07012	0.77	18.32	0	138
HCP	320.85	164.68	1.2363	75.32	12.61	0	142
HTC-HCP	167.98	80.34	0.3019	13.34	0.21	4.98	124

188

189 **Fig. 3** shows N₂ adsorption-desorption isotherms and pore-size distribution of HTC-HCP and
 190 structural properties of pore surfaces for all the materials at 77 K. As **Table 1** shown, CM-PS has low
 191 BET surface area (40.25 m²/g) and pore volume (0.07012 cm³/g). While the BET surface area (320.85
 192 m²/g) and pore volume (1.2363 cm³/g) of HCP significantly increase after the Friedel-Crafts reaction,
 193 demonstrating that the reaction can greatly improve the pore structure of the polymers. However,
 194 when HTC is uploaded on the surface of HCP, the BET surface area and pore volume decrease to
 195 167.98 m²/g and 0.3019 cm³/g, respectively, implying blockage of some pores with the added functional
 196 groups [34] (**Fig. 3a**). Based on the IUPAC classification [35], the N₂ adsorption of HTC-HCP belongs
 197 to type II. It significantly increases at the relative pressure ($P/P^{\circ} = 0$ to 0.05), and steadily rises at the
 198 pressure of $0.1 < P/P^{\circ} < 0.9$ and rapidly climbs in the range of $P/P^{\circ} > 0.9$ (**Fig. 3b**), implying that
 199 some micropores and mesopores ranging 10-50 nm mostly exist in HTC-HCP [36, 37].
 200

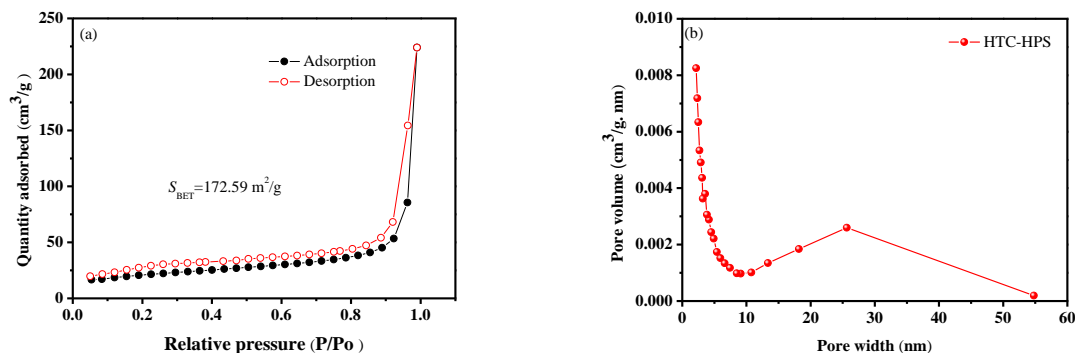


Fig. 3. (a) Adsorption–desorption isotherms of N₂ at 77 K and (b) pore-size distribution of HTC-HCP.

3.2. Adsorption performance of HTC-HCP

HTC-HCP has adsorption ability for a wide variety of organic compounds such as amines, phenols, and dyes from aqueous solutions, and the adsorption curves of amines, phenols, and dyes are shown in Fig. 4.

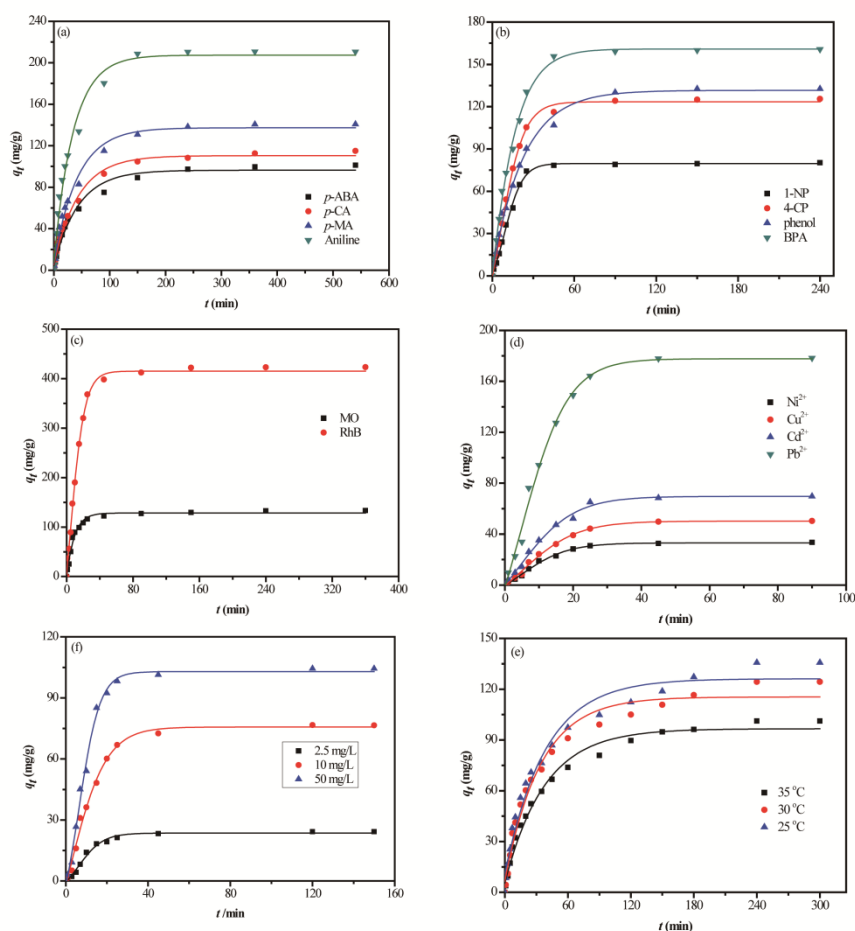
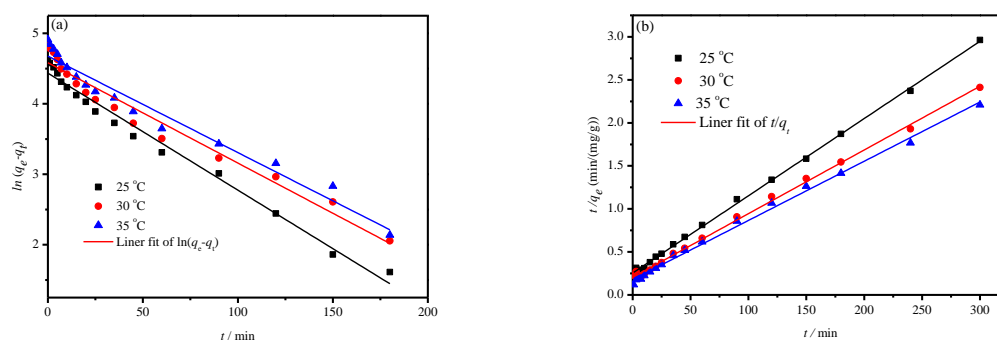


Fig. 4. Adsorption curves of HTC-HCP for (a) amines, phenols (b), dyes (c), and (d) metal ions (Ni²⁺, Cu²⁺, Cd²⁺, and Pb²⁺) at 25 °C (0.1 g, pH = 7, 100 mL of 100 mg/L solution, and 200 rpm). e) Effect of temperature on the adsorption capacity of aniline from aqueous solution (0.1 g, pH = 7, 100 mL, 80 mg/L, and 200 rpm). f) Adsorption capacity for aniline with various concentration (2.5, 10, and 70 mg/L) at 30 °C (0.01 g HTC-HCP, pH = 7, and 200 rpm).

215 **Fig. 4a** displays that the adsorption capacity of amines (aniline, *p*-MA, *p*-CA, and *p*-ABA)
 216 increases quickly in the first 100 min, and then gradually gets to equilibrium. Adsorption
 217 equilibrium is reached about in 250 min for aniline, *p*-MA, *p*-CA, and *p*-ABA. Further increase of
 218 contact time has a negligible effect on the equilibrium adsorption capacity of the amines. The
 219 maximum adsorption capacity for *p*-ABA, *p*-CA, *p*-MA, and aniline is 101.12, 115.98, 140.75, and
 220 210.59 mg/g, respectively. The polymer also adsorbs other organic contaminants such as dyes and
 221 phenol compounds from wastewater. The maximum adsorption capacity for 1-NP, 4-CP, phenol,
 222 and BPA is 80.24, 125.52, 132.64, and 160.73 mg/g, respectively, in 120 min. The adsorption
 223 equilibrium for RhB and MO is observed in 160 and 240 min, respectively, and their adsorption
 224 capacity is 133.46 and 423.22 mg/g, respectively, which is higher than some the previously reported
 225 adsorbents [38-41]. The results implied that HTC-HCP has good potential applications for the
 226 removal of various organic contaminants from wastewater.

227 HTC-HCP can also capture various metal ions fast and effectively from aqueous solution (**Fig.**
 228 **4d**). The adsorption capacity of Ni²⁺, Cu²⁺, Cd²⁺, and Pb²⁺ is 33.46, 50.33, 69.69, and 178.27 mg/g after
 229 30, 45, 45, and 80 min, respectively, at 25 °C. The adsorption capacity of HTC-HCP is higher than
 230 some commonly used adsorbents such as chitosan, activated carbon and newly developed
 231 adsorbents (**Table S1**). It suggests that HTC-HCP is a promising sorbent in the removal of metal
 232 ions.

233 To understand the adsorption, aniline is applied as the model adsorbate, and adsorption
 234 experiment is performed in detail. The removal efficiency of HTC-HCP for aniline is studied at 25,
 235 30, and 35 °C, respectively (**Fig. 4e**). The adsorption capacity increases rapidly in 100 min and then
 236 gradually reaches equilibrium for 101.21, 124.37, and 135.75 mg/g about in 240 min, respectively.
 237 Further increase of contact time has no significant effect on the adsorption equilibrium. Higher
 238 temperature decreases adsorption equilibrium time because of the faster molecular motion, but
 239 results in a lower absorption capacity due to the exothermic process during the absorption process
 240 of aniline. Effect of initial aniline concentration on the adsorption capacity of HTC-HCP is also
 241 investigated at different concentrations, which are 2.5, 10, and 50 mg/L, respectively, at 25 °C. The
 242 corresponding adsorption capacity is 24.22, 89.52, and 160.23 mg/g, respectively. When the
 243 adsorption is performed with 2.5 mg/L at 25 °C, the removal rate of aniline is above 95% in 40 min.
 244 The results indicate HTC-HCP may be used in the wastewater treatment with very low
 245 concentration of aniline. In order to elucidate the adsorption mechanism, the adsorption data of
 246 aniline are analysed with the pseudo-first-order and pseudo-second-order kinetic models in
 247 **supplementary information**, and the results are displayed in **Fig. 5**. **Table 2** shows that the
 248 correlation coefficient for the pseudo-second-order kinetic model ($R^2 > 0.99$) is higher than that of the
 249 pseudo-first-order kinetic model ($R^2 < 0.99$), indicating that the adsorption process fitted by the
 250 pseudo-second-order kinetic model is more reasonable. Furthermore, the theoretical calculated
 251 values ($q_{e,cal}$) obtained from the pseudo second-order model are in good agreement with the
 252 experimental values ($q_{e,exp}$), implying the model better describe the adsorption behavior of aniline
 253 onto HTC-HCP. The results show that the chemical adsorption may be involved in the adsorption
 254 process [42, 43].



255 **Fig. 5.** Linear regressions of kinetics plots (a) pseudo-first-order model, and (b) pseudo-second-order
 256 model.

257
258**Table 2.** Adsorption kinetics parameters for aniline on HTC-HCP.

Model	Parameter	Temperature/°C		
		25	30	35
pseudo-first-order	$q_{e,exp}$ (mg/g)	135.75	124.37	101.21
	k_1 (min^{-1})	0.01369	0.01425	0.01660
	$q_{e,cal}$ (mg/g)	107.35	97.87	84.33
	R^2	0.984	0.962	0.964
pseudo-second-order	k_2 (g/mg/min)	0.006880	0.007402	0.008981
	$q_{e,cal}$ (mg/g)	145.34	135.09	111.35
	R^2	0.998	0.997	0.996

259
260
261
262
263
264
265
266
267
268
269
270
271
272

Aniline is further used to evaluate the equilibrium adsorption of HTC-HCP. **Fig.6** displays the adsorption isotherms of aniline at 25, 30, and 35 °C, respectively. Adsorption amount of aniline increases with the increasing the initial concentration until the maximum adsorption is reached. For the compound, adsorption amount decrease with the rising temperature, implying the adsorption is an exothermic process and higher temperature is unfavorable for the adsorption. Langmuir, Freundlich, and D-R models are used to analyze the equilibrium adsorption data of aniline on the HTC-HCP and are given in [supplementary information \[37, 44\]](#). **Table 3** shows that the Freundlich model has a better fit to the experimental data than the Langmuir model because of higher R^2 , suggesting that the adsorption of aniline onto HTC-HCP should be a multilayer process [28]. From **Table 3**, K_i values calculated from the Freundlich model increase with the increasing temperature, but n values decrease with the rising temperatures for the compound onto the HTC-HCP and are greater than 1 at all the temperature studied, implying that aniline are favorably adsorbed by HTC-HCP [45].

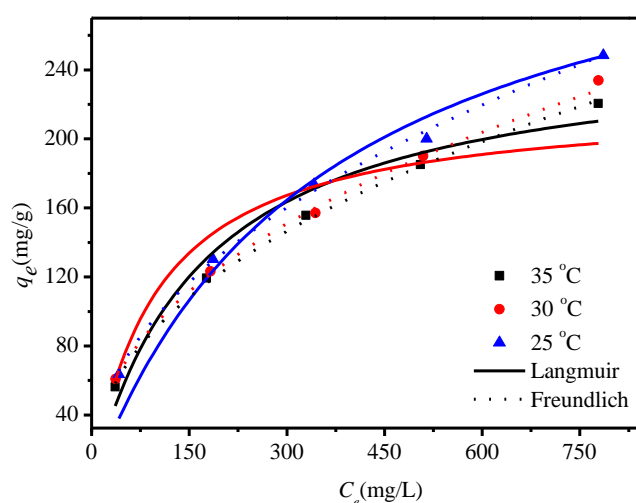
273
274
275
276

Fig. 6. Adsorption isotherms and fitted data of aniline on the HTC-HCP at 25, 30, and 35 °C, respectively. Each point represents the average of three replicates (\pm standard deviation, 5%). Adsorption conditions: HTC-HCP (0.1 g), V_0 (100 mL), pH = 7, 200 r/min, 720 min.

277
278
279**Table 3.** The correlated parameters for the adsorption of aniline via HTC-HCP according to Langmuir, Freundlich, and D-R models

Model	Temperature (°C)	Parameter	
Langmuir Model	25	K_L (L/mg)	5.89×10^{-3}
		q_m (mg/g)	361.18
		R^2	0.986
	30	K_L (L/mg)	1.01×10^{-2}
		q_m (mg/g)	302.58
		R^2	0.988
	35	K_L (L/mg)	2.79×10^{-3}
		q_m (mg/g)	256.17
		R^2	0.963
Freundlich Model	25	K_f (L/mg)	9.10
		$1/n$	0.24
		R^2	0.994
	30	K_f (L/mg)	10.67
		$1/n$	0.32
		R^2	0.993
	35	K_f (L/mg)	11.99
		$1/n$	0.40
		R^2	0.997
D-R Model	25	β	2.98×10^{-4}
		q_m (mg/g)	128.68
		E_a (kJ/mol)	42.05
	30	R^2	0.673
		β	2.80×10^{-4}
		q_m (mg/g)	114.89
	35	E_a (kJ/mol)	28.87
		R^2	0.498
		β	2.70×10^{-4}
	q_m (mg/g)	107.48	
	E_a (kJ/mol)	24.98	
	R^2	0.836	

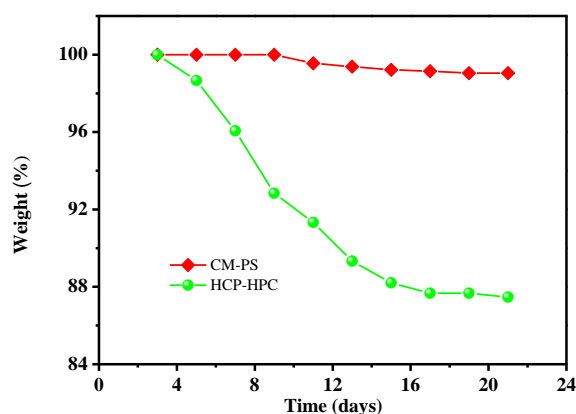
280
281
282

Table S2 shows that the negative ΔH° demonstrates the exothermic nature of the adsorption process for aniline on HTC-HCP, which is supported by the decrease of aniline adsorption with the

283 increase in temperature. The negative ΔG° implies that the adsorption process is spontaneous,
 284 indicating a higher preference of aniline onto the HTC-HCP at lower temperature. Besides, the
 285 positive ΔS values reveal that the adsorption process is an entropy increase process.

286 3.3. Biodegradation test and reuse experiments

287 As shown in Fig. 7, biodegradation experiments displayed that CM-PS
 288 was almost non-degradable, but HTC-HCP gained a certain degree of biodegradability (about 12.4
 289 wt%), implying that it can effectively reduce the damage to the environment. In addition, HTC-HCP
 290 was used repeatedly for five adsorption-desorption cycles (Figure S2) to test its stability and
 291 reusability, the equilibrium capacity remained unchanged, confirming that HTC-HCP could be
 292 efficiently recovered and it exhibited a good regeneration property.
 293

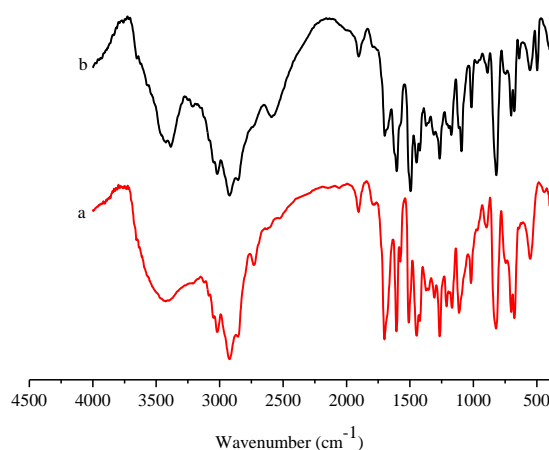


294

295 **Fig. 7.** Weight lost of CM-PS and HTC-HCP after biodegradation.

296 3.4. Adsorption mechanism

297 To demonstrate the adsorption mechanism, FTIR spectra of HTC-HCP and HTC-HCP after
 298 adsorption of aniline was investigated (Fig. 8). In the FTIR spectra of Fig. 8, the IR band in the
 299 3300-3500 cm^{-1} region is due to the -OH stretching mode. After adsorption, the band is slightly
 300 weakened in intensity and is red-shifted by 5-15 cm^{-1} , implying the presence of strong affinities
 301 between HTC-HCP and aniline compounds. The result shows that the weak interactions of the -OH
 302 or -COOH functional groups of the HTC-HCP with aniline compounds formed during the
 303 adsorption process.
 304
 305

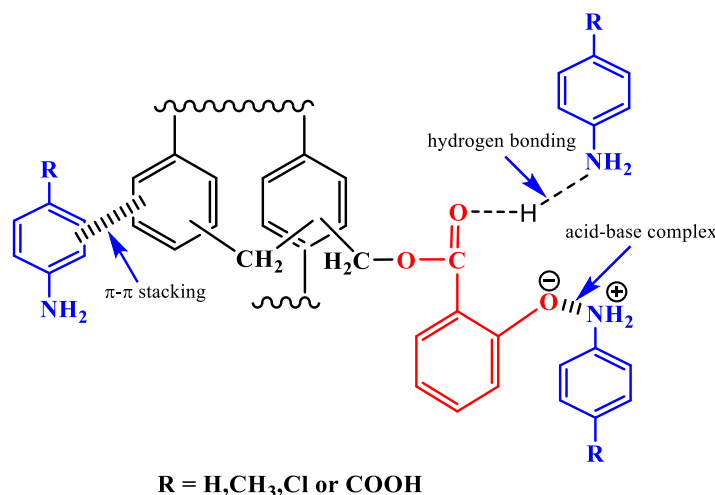


306

307

Fig.8. FTIR spectra of (a) HTC-HCP; (b) after aniline adsorption.

308 When HCP is grafted onto the surface of HCP, the two functional groups of HCP
 309 such as carboxyl group and hydroxyl group on the surface of HTC-HCP are maintained, which
 310 could form acid-base interaction and hydrogen bonding interaction between HTC molecule and
 311 HTC-HCP. However, the hydrogen bonding interaction between HTC and the aniline compound is
 312 regarded as a dominant attractive force. In order to evaluate the weak interaction, the binding
 313 energies of HTC and aniline have been calculated using the local density approximation (LDA) in
 314 the Perdew-Wang (PWC) form at the DND basis set level (Supporting Information), which was used
 315 in previous report [46, 47]. As shown in Figure S4 and Table S5, the results demonstrate that HTC
 316 form stable complex with aniline. The complex can significantly increase the adsorption amount of
 317 aniline. In the process of the compound adsorbed by HTC-HCP in aqueous solution, the NH₂ group
 318 of the adsorbate and the -CO- and -OH groups of the adsorbent can form N-H...O and O-H...O
 319 hydrogen bonding interactions. In addition, the π - π conjugation and acid-base complex also can
 320 play an important role in the adsorption process of aniline, according to previous reports [46, 48]. As
 321 shown in Scheme 2, it was clear that the significant improvement of adsorption of aniline by
 322 HTC-HCP was driven by the synergistic effects of weak interactions such as π - π stacking,
 323 hydrogen bonding, and acid-base complex.
 324



325

326 **Scheme 2.** Schematic mechanism of the adsorption of aniline compounds with HTC-HCP.

327 4. Conclusion

328 A HTC-modified hyper-crosslinked polymer (HTC-HCP) is successfully synthesized, and used
 329 to assess the capacities for removal of organic contaminants and heavy metal ions from wastewater.
 330 The introduction of HTC onto the surface of HCP significantly enhances the adsorption of the
 331 pollutants, and the synergistic effects of weak interactions play an important role. The equilibrium
 332 adsorption amounts are 101.12, 115.98, 140.75, and 210.59 mg/g for *p*-ABA, *p*-CA, *p*-MA, and aniline,
 333 respectively, which are more than most adsorbents in the literature. The adsorption kinetic data of
 334 four aniline are well fitted with the pseudo-second-order kinetic model. The adsorption isotherms of
 335 aniline can be fitted better to the Freundlich model. Adsorption mechanism indicates that formation
 336 of chemical bonding via π - π stacking, acid-base interaction, and hydrogen bonding plays a crucial
 337 role in the enhanced adsorption of aniline. Moreover, biodegradation experiments show that
 338 HTC-HCP is an environmentally friendly adsorbent. In short, the present adsorption material
 339 exhibits great potential for the application in water treatment.

340 **Supplementary Materials:** The following are available online at <http://www.mdpi.com/>

341 **Author Contributions:** Methodology, validation, investigation, writing, Z. J. Yang; data curation,
 342 Investigation, original draft preparation, Q. R. Li; J.W. Chen; data curation; funding acquisition,
 343 project administration, writing-review and editing, H. B. Ji.

344 **Funding:** This work was preliminarily supported by the National Natural Science Foundation of
 345 China (21425627, 21376279), National Natural Science Foundation of China-SINOPEC Joint
 346 fund (U1663220), Natural Science Foundation of Guangdong Province (2017A030313057), and

347 Guangdong Technology Research Center for Synthesis and Separation of Thermosensitive
348 Chemicals (2015B090903061) for providing financial support to this project.

349 **Conflicts of Interest:** The authors declare that they have no conflict of interest

350 References

- 351 1. Chen, C.; Geng, X.; Huang, W. Adsorption of 4-chlorophenol and aniline by nanosized activated
352 carbons. *Chem Eng J* **2017**, *327*, 941-952.
- 353 2. Zhao, B.; Jiang, H.; Lin, Z.; Xu, S.; Xie, J.; Zhang, A. Preparation of acrylamide/acrylic acid cellulose
354 hydrogels for the adsorption of heavy metal ions. *Carbohydr Polym* **2019**, *224*, 115022.
- 355 3. Wee, L.; Janssens, N.; Vercammen, J.; Tamaraschi, L.; Thomassen, L. J.; Martens, J. Stable TiO₂-USY
356 zeolite composite coatings for efficient adsorptive and photocatalytic elimination of geosmin from
357 water. *J Mater Chem A* **2015**, *3*, 2258-2264.
- 358 4. Ye, Y.; Wan, D.; Du, J.; Jin, M.; Pu, H. Dendritic amphiphile mediated porous monolith for
359 eliminating organic micropollutants from water. *J Mater Chem A* **2015**, *3*, 6297-6300.
- 360 5. Fakhre, N. A.; Ibrahim, B. M. The use of new chemically modified cellulose for heavy metal ion
361 adsorption. *J Hazard Mater* **2018**, *343*, 324-331.
- 362 [6] Chao, H. P.; Lee, C. K.; Juang, L. C.; Han, Y. L. Sorption of organic compounds, oxyanions, and
363 heavy metal ions on surfactant modified titanate nanotubes. *Ind Eng Chem Res* **2013**, *52*, 9843-9850.
- 364 7. Benito, A.; Penades, A.; Lliberia, J. L.; Gonzalez-Olmos, R. Degradation pathways of aniline in
365 aqueous solutions during electro-oxidation with BDD electrodes and UV/H₂O₂ treatment.
366 *Chemosphere* **2017**, *166*, 230-237.
- 367 8. Chai, K.; Ji, H. Dual functional adsorption of benzoic acid from wastewater by biological-based
368 chitosan grafted β -cyclodextrin. *Chem Eng J* **2012**, *203*, 309-318.
- 369 9. Li, B.; Su, F.; Luo, H. K.; Liang, L.; Tan, B. Hypercrosslinked microporous polymer networks for
370 effective removal of toxic metal ions from water. *Micropor Mesopor Mat* **2011**, *138*, 207-214.
- 371 10. Kolbasov, A.; Sinha-Ray, S.; Yarin, A. L.; Pourdeyhimi, B. Heavy metal adsorption on
372 solution-blown biopolymer nanofiber membranes. *J Membrane Sci* **2017**, *530*, 250-263.
- 373 11. Gao, D. W.; Hu, Q.; Pan, H.; Jiang, J.; Wang, P. High-capacity adsorption of aniline using surface
374 modification of lignocellulose-biomass jute fibers. *Bioresour Technol* **2015**, *193*, 507-512.
- 375 12. Morin-Crini, N.; Winterton, P.; Fourmentin, S.; Wilson, L. D.; Fenyvesi, É.; Crini, G.
376 Water-insoluble β -cyclodextrin-epichlorohydrin polymers for removal of pollutants from aqueous
377 solutions by sorption processes using batch studies: A review of inclusion mechanisms. *Prog Polym*
378 *Sci* **2018**, *78*, 1-23.
- 379 13. Bruzzoniti, M. C.; Appendini, M.; Rivoira, L.; Onida, B.; Del Bubba, M.; Jana, P.; Sorarù, G. D.
380 Polymer-derived ceramic aerogels as sorbent materials for the removal of organic dyes from
381 aqueous solutions. *J Am Ceram Soc* **2018**, *101*, 821-830.
- 382 14. Yin, L.; Fan, X.; Jia, X.; Zhang, B.; Zhang, H.; Zhang, A.; Zhang, Q. Hypercrosslinked polymers:
383 controlled preparation and effective adsorption of aniline. *J Mater Sci* **2016**, *51*, 8579-8592.
- 384 15. Huang, J.; Zha, H.; Jin, X.; Deng, S. Efficient adsorptive removal of phenol by a
385 diethylenetriamine-modified hypercrosslinked styrene-divinylbenzene (PS) resin from aqueous
386 solution. *Chem Eng J* **2012**, *195-196*, 40-48.
- 387 16. Yang, Z.; Huang, X.; Yao, X.; Ji, H. Thiourea modified hyper-crosslinked polystyrene resin for
388 heavy metal ions removal from aqueous solutions. *J Appl Polym Sci* **2017**, *135*, 1-8.
- 389 17. Huang, J.; Turner, S. R. Hypercrosslinked polymers: A Review. *Polym Rev* **2018**, *58*:1-41.
- 390 18. Fontanals, N.; Marcé, R. M.; Borrull, F.; Cormack, P. A. G. Hypercrosslinked materials:
391 preparation, characterisation and applications. *Polym Sci* **2015**, *6*, 7231-7244.
- 392 19. He, C.; Huang, J.; Yan, C.; Liu, J.; Deng, L.; Huang, K. Adsorption behaviors of a novel carbonyl
393 and hydroxyl groups modified hyper-cross-linked poly(styrene-co-divinylbenzene) resin for
394 β -naphthol from aqueous solution. *J Hazard Mater* **2010**, *180*, 634-639.
- 395 20. Wang, X.; Dai, K.; Chen, L.; Huang, J.; Liu, Y. N. An ethylenediamine-modified hypercrosslinked
396 polystyrene resin: Synthesis, adsorption and separation properties. *Chem Eng J* **2014**, *242*, 19-26.
- 397
- 398 21. Kuang, W.; Li, H.; Huang, J.; Liu, Y. N. Tunable porosity and polarity of the polar
399 hyper-cross-linked resins and the enhanced adsorption towards phenol. *Ind Eng Chem Res* **2016**, *55*,
400 12213-12221.

- 401 22. Jin, N. R.; Xie, P. Z.; Zhang, J. T.; Sun, G.; Hu, Y. H.; Zhao, D. M. Synthesis of high-purity
402 2-hydroxyterephthalic acid. *Chem Ind Eng Pro* **2011**, *30*, 1789-1794.
- 403 23. Wang, X. M., Mao, X., Huang, J. H. Hierarchical porous hyper-cross-linked polymers modified
404 with phenolic hydroxyl groups and their efficient adsorption of aniline from aqueous solution.
405 *Colloids Surf A Physicochem Eng Asp* **2018**, *558*, 80-87.
- 406 24. Kuang, W.; Liu, Y.N.; Huang, J. Phenol-modified hyper-cross-linked resins with almost all
407 micro/mesopores and their adsorption to aniline. *J Colloid Interf Sci* **2017**, *487*, 31-37.
- 408 25. Caldwell, J. R.; Moyer, H. V. Determination of chloride: a modification of the volhard method.
409 *Ind Eng Chem Res* **1935**, *7*, 447-450.
- 410 26. Wang, G.; Zhang, C.; Guo, X.; Ren, Z. FTIR and molecular mechanics studies of H-bonds in
411 aliphatic polyurethane and polyamide-66 model molecules. *Spectrochim Acta A* **2008**, *69*, 407-412.
- 412 27. Wang, X.; Zhang, T.; Huo, J.; Huang, J.; Liu, Y.-N. Tunable porosity and polarity of polar
413 post-cross-linked resins and selective adsorption. *J Colloid Interf Sci* **2017**, *487*, 231-238.
- 414 28. Ling, X.; Li, H.; Zha, H.; He, C.; Huang, J. Polar-modified post-cross-linked polystyrene and its
415 adsorption towards salicylic acid from aqueous solution. *Chem Eng J* **2016**, *286*, 400-407.
- 416 30. Lu, K.; Chai, K.; Liang, Q.; Xu, Z.; Li, G.; Ji, H. Biosorption and selective separation of
417 acetophenone and 1-phenylethanol with polysaccharide-based polymers. *Chem Eng J* **2017**, *317*,
418 862-872.
- 419 31. Wan, Y. J.; Tang, L. C.; Yan, D.; Zhao, L.; Li, Y. B.; Wu, L. B.; Jiang, J. X.; Lai, G. Q. Improved
420 dispersion and interface in the graphene/epoxy composites via a facile surfactant-assisted process.
421 *Compos Sci Technol* **2013**, *82*, 60-68.
- 422 32. Liu, G.; Wang, Y.; Shen, C.; Ju, Z.; Yuan, D. A facile synthesis of microporous organic polymers
423 for efficient gas storage and separation. *J Mater Chem A* **2015**, *3*, 3051-3058.
- 424 33. Wang, D.; Li, X.; Jin, X.; Jia, Q. Design of cucurbit[6]uril-based hypercrosslinked polymers for
425 efficient capture of albendazole. *Sep Purif Technol* **2019**, *216*, 9-15.
- 426 34. Shao, L.; Li, Y.; Zhang, T.; Liu, M.; Huang, J. Controllable synthesis of polar modified
427 hyper-cross-linked resins and their adsorption of 2-naphthol and 4-hydroxybenzoic acid from
428 aqueous solution. *Ind Eng Chem Res* **2017**, *56*, 2984-2992.
- 429 35. Thommes, M.; Kaneko, K.; Neimark, A. V.; Olivier, J. P.; Rodriguezreinoso, F.; Rouquerol, J.; Sing,
430 K. S. W. Physisorption of gases, with special reference to the evaluation of surface area and pore size
431 distribution (IUPAC Technical Report). *Pure Appl Chem* **2016**, *38*, 25-25.
- 432 37. Jiang, X.; Huang, J. Adsorption of Rhodamine B on two novel polar-modified post-cross-linked
433 resins: Equilibrium and kinetics. *J Colloid Interf Sci* **2016**, *467*, 230-238.
- 434 38. Khaniabadi, Y. O.; Heydari, R.; Nourmoradi, H.; Basiri, H.; Basiri, H. Low-cost sorbent for the
435 removal of aniline and methyl orange from liquid-phase: Aloe vera leaves wastes. *J Taiwan Inst Chem*
436 *E* **2016**, *68*, 90-98.
- 437 39. Hao, Z.; Wang, C.; Yan, Z.; Jiang, H.; Xu, H. Magnetic particles modification of coconut
438 shell-derived activated carbon and biochar for effective removal of phenol from water. *Chemosphere*
439 **2018**, *211*, 962-969.
- 440 40. Kooh, M. R.R.; Dahri, M. K.; Lim, L. B. L. The removal of rhodamine B dye from aqueous solution
441 using Casuarina equisetifolia needles as adsorbent. *Cogent Environ Sci* **2016**, *2*, 1140553.
- 442 41. Robati, D.; Mirza, B.; Rajabi, M.; Moradi, O.; Tyagi, I.; Agarwal, S.; Gupta, V. K. Removal of
443 hazardous dyes-BR 12 and methyl orange using graphene oxide as an adsorbent from aqueous
444 phase. *Chem Eng J* **2016**, *284*: 687-697.
- 445 42. Ho, Y.S.; Mckay, G. Pseudo-second order model for sorption processes. *Process Biochem* **1999**, *34*,
446 451-465.
- 447 43. Yang, Z.; Miao, H.; Rui, Z.; Ji, H. Enhanced formaldehyde removal from air using fully
448 biodegradable chitosan grafted β -cyclodextrin adsorbent with weak chemical interaction. *Polymers*
449 **2019**, *11*, 276.
- 450 44. Wang, X.; Deng, R.; Jin, X.; Huang, J. Gallic acid modified hyper-cross-linked resin and its
451 adsorption equilibria and kinetics toward salicylic acid from aqueous solution. *Chem Eng J* **2012**, *191*,
452 195-201.
- 453 45. Chingombe, P.; Saha, B.; Wakeman, R. J. Sorption of atrazine on conventional and surface
454 modified activated carbons. *J Colloid Interf Sci* **2006**, *302*, 408-416.

- 455 46. Yang, Z.; Zeng, H.; Zhou, X.; Ji, H. Mechanism into selective oxidation of cinnamaldehyde using
456 β -cyclodextrin polymer as phase-transfer catalyst. *Tetrahedron* **2012**, *68*, 5912-5919.
- 457 47. Yang, Z. J.; Zeng, H.; Zhou, X. T.; Ji, H. B. Enhanced catalytic activity and recyclability for
458 oxidation of cinnamaldehyde catalysed by β -cyclodextrin cross-linked with chitosan. *Supramol Chem*
459 **2013**, *25*, 233-245.
- 460 48. Yang, Z.; Ji, H. 2-Hydroxypropyl- β -cyclodextrin polymer as a mimetic enzyme for mediated
461 synthesis of benzaldehyde in water. *ACS Sustain Chem Eng* **2013**, *1*, 1172-1179.
462